RESTRICTED CONFIDENTIAL

CONFIDENTIAL

Copy 6
RM L50H23

NACA RM L50H23

CLASSIFICATION CHANGED

OCT 16 1950

UNCLASSIFIED

To RESTRICTED

By authority

NACA

RESEARCH MEMORANDUM

PRELIMINARY EMPIRICAL DESIGN REQUIREMENTS FOR THE PREVENTION OF TUMBLING OF AIRPLANES HAVING NO HORIZONTAL TAILS

FOR REFERENCE

NOT TO BE TAKEN FROM THIS ROOM

By Robert L. Bryant

Langley Aeronautical Laboratory
Langley Air Force Base, Va.

CLASSIFICATION CANCELLED

Authority NACA R7 2560 Date 8/23/54

By NASA 9/8/54 See

CLASSIFICATION CHANGED

To Confidential

By authority of Date 12/8/53

NATIONAL ADVISORY COMMITTEE FOR AERONAUTICS

WASHINGTON

October 11, 1950

UNCLASSIFIED

CONFIDENTIAL

RESTRICTED

NATIONAL ADVISORY COMMITTEE FOR AERONAUTICS

RESEARCH MEMORANDUM

PRELIMINARY EMPIRICAL DESIGN REQUIREMENTS FOR THE PREVENTION OF TUMBLING OF AIRPLANES HAVING NO HORIZONTAL TAILS

By Robert L. Bryant

SUMMARY

An investigation has been made of the design characteristics and loadings that are conducive to the tumbling of airplanes that have no horizontal tails. Preliminary empirical design requirements based on model tests of 18 different configurations are presented. A brief explanation of the phenomenon of tumbling is appended.

INTRODUCTION

The summary of results of tumbling investigations of several dynamic models to determine their tumbling characteristics (reference 1) indicated that tumbling may occur only for airplanes having no horizontal tails and that the degree of static longitudinal stability was indicative of the proneness of an airplane to tumble. From analysis of the data of reference 1 and of additional data obtained in the present investigation certain empirical design requirements for the prevention of tumbling of horizontal tailless airplanes were indicated and are presented herein. Results were also obtained in the present investigation from tumbling tests of five flat plates. Tumble theory advanced by Dupliech in reference 2 is also discussed and appended herein. Although further research will be necessary for complete solution of the problem, it appeared desirable to present an empirical criterion at this time based on existing knowledge.

SYMBOLS

All angles and vectorial quantities are shown in figure 1.

ξ distance measured along the horizontal earth axis, feet

ζ	distance measured along the vertical earth axis, feet
α	angle of attack, degrees
γ	flight-path angle relative to ξ earth axis, degrees
θ	angular displacement in pitch with respect to the earth ξ axis, degrees
$\bar{q}$	average rate of pitch during any cycle of the tumble after equilibrium has been obtained, radians per second
q	instantaneous rate of pitch, radians per second
V	instantaneous resultant velocity, feet per second
a_t	acceleration tangent to flight path, feet per second^2
a_n	acceleration normal to flight path, feet per second^2
t	time, seconds
m	mass, slugs
W	weight, pounds
I_Y	moment of inertia about the lateral axis, slug-feet^2
S	wing area, feet^2
b	wing span, feet
c	wing chord at any station, feet
$\bar{c}$	mean aerodynamic chord, feet
h	distance from center of gravity to centroid of plan-form area, feet
ρ	air density, slug per cubic foot
μ_b	relative-density coefficient based on span $\left(\frac{m}{\rho Sb}\right)$
R_A	resultant aerodynamic force, pounds
R_I	resultant inertia force, pounds

L lift, pounds

D drag, pounds

M pitching moment, foot-pounds

C_L lift coefficient $\left(\frac{\text{Lift}}{\frac{1}{2}\rho V^2 S}\right)$

C_M pitching-moment coefficient $\left(\frac{\text{Pitching moment}}{\frac{1}{2}\rho V^2 S\bar{c}}\right)$

C_N normal-force coefficient $\left(\frac{\text{Normal force}}{\frac{1}{2}\rho V^2 S}\right)$

C_X longitudinal-force coefficient $\left(\frac{\text{Longitudinal force}}{\frac{1}{2}\rho V^2 S}\right)$

Parenthetic subscripts:

$(\ )_\alpha$ due to angle of attack

$(\ )_{\dot{\alpha}}$ due to time rate of change of angle of attack

$(\ )_q$ due to pitching velocity

APPARATUS AND TESTS

Models

The models were scaled from full-scale airplanes with the exception of two research models G and I and five flat plates, models N, O, P, Q, and R, which were built to an arbitrary scale. The dimensional characteristics, mass characteristics, pitching-moment characteristics, and plan views of the models are given in tables I and II in terms of full-scale values. The models were made of balsa and ballasted with lead weights to obtain dynamic similarity to their actual or assumed full-scale counterparts at some arbitrary altitude as indicated on table II. The assumed full-scale counterparts of the research models and flat plates were such that their spans were within the range of the other models tested.

Wind Tunnel and Testing Technique

The tumble tests were conducted in the Langley 20-foot free-spinning tunnel, a vertical wind tunnel of dodecagonal cross section capable of airspeeds up to approximately 60 miles per hour and is similar to the former Langley 15-foot free-spinning tunnel as described in reference 3. For the tests, two methods of launching the models were employed: the model was released from a nose-up attitude to simulate a whip stall in order to determine whether the model would start tumbling of its own accord, or the model was launched with initial pitching rotation in order to determine whether the model would continue to tumble once the tumbling motion had been started. The simulated whip stall was obtained by holding the model in the air stream with its nose up and simply letting go of the model. When launched with initial pitching rotation, the model was held in the air stream and forced to rotate by applying a torque about the lateral axis as it was launched.

The models were generally tested with three elevator deflections, full up, neutral, and full down with both positive and negative initial pitching rotation. Whip-stall tests were generally made only for those conditions for which the model tumbled when given forced rotation. It was considered that the model would tumble for a particular center-of-gravity location if a tumble was obtained by any method of launching for any elevator position.

Parameters Considered for Empirical Criterion

The results of the investigations summarized in reference 1 indicated that aspect ratio, the square of the radius of gyration in percent of the span squared and the degree of static longitudinal stability appeared to be important parameters with regard to tumbling. When in the analysis of available data and data obtained in the present investigation no way of using these parameters was found that would fit into the scheme of separating the tumbles from no tumbles, it was decided to look for parameters whose effect on the tumble were most obvious. Variation of the center-of-gravity location has a decided effect on tumble results. The center-of-gravity location determines the degree of static longitudinal stability which, in conjunction with the moment of inertia, determines the initial rate of pitch. Since the rate of pitch, which, in the case of tumbling is equal to the rate of change of angle of attack, determines the amount of hysteresis in lift (see appendix), it was decided to consider the center-of-gravity location in percent of the mean aerodynamic chord as a basic parameter. The effect of the damping moment is quite obvious inasmuch as conventional-type models (with horizontal tails) which have a large degree of damping will not tumble even when the center-of-gravity location is such that extreme static instability exists. If the damping moment always exceeds the moment

due to hysteresis in lift for any rate of change of angle of attack, the tumbling motion can never get started. The usual expression for wing damping which considers only relatively small rates of pitch may not be applicable for tumbling motions in which the rates of pitch are appreciably larger. It was felt that some measure of the damping would be indicated by the square of the distance between the center of gravity and the centroid of the plan-form area. Damping, in addition to being a function of the rate of pitch, is also a function of the rate of descent; the rates of pitch and descent are respectively dependent upon moment of inertia and mass, and therefore it was felt that the ratio of mass to moment of inertia, or radius of gyration squared should also appear in the damping parameter. The expression $\frac{h^2}{I_Y/m}$ or $\frac{mh^2}{I_Y}$ was thus chosen to represent damping.

RESULTS

The results of the tumbling investigation for the 11 specific models and the 2 research models are presented in figures 2 and 3. Figure 2 presents the results of tests of models having aspect ratios greater than 3 and varying up to 11, whereas figure 3 presents the results of tests of models having aspect ratios of 3 or less. The results of the tumbling tests of the flat plates are shown in figure 4. The coordinates on the figures are the two parameters previously discussed, center-of-gravity position and mh^2/I_Y. Results for both forced rotations and for whip stalls are shown.

Interpretation of model tumbling results as applied to corresponding full-scale airplanes regarding the possibility of tumbling is as follows: If a model does not tumble when launched with forced rotation, the corresponding airplane will not tumble; if the model tumbles when launched with forced rotation the corresponding airplane may tumble but there will be greater likelihood of tumbling if the model tumbles when launched from a whip stall.

DISCUSSION

Where data permitted, two separation lines have been drawn in figures 2 to 4 to separate the data for the models which tumbled when given forced rotation from the data for the models which tumbled from a whip stall and from the data for the models which did not tumble. In addition, a line has been drawn, where possible, below which tumbles from a whip stall appear unlikely. The dashed lines are conjectural and have been drawn on the assumption that the separation lines are a family of curves as some function of aspect ratio.

Tumbling tendencies of nine models whose aspect ratios were greater than 3 and ranging up to 11 are indicated in figure 2. At a given value of the parameter mh^2/I_Y, the models would not tumble even when launched with forced rotation for relatively forward center-of-gravity positions. As the center of gravity was moved rearward, tumbles were obtained first only from forced rotation, then from forced rotation and occasionally from whip stalls, and finally it appeared likely that tumbles would always be obtained even from whip stalls for rearward center-of-gravity positions. At a forward center-of-gravity position, increasing the value of mh^2/I_Y tended to decrease the tumbling tendency from forced rotation, whereas for a rearward center-of-gravity position the tendency to tumble from whip stalls was increased for an increase in mh^2/I_Y. This difference in effect of mh^2/I_Y may be partially attributable to a difference in rotational inertia. Large radius of gyration (high inertia with low mass) would tend to prevent the tumbling motion from a whip stall, whereas once the tumbling motion has been obtained from forced rotation, it would aid in sustaining the motion.

These results indicate that the center of gravity need not be nearly so far forward to avoid tumbles from whip stalls as it must be to avoid tumbles from forced rotation at low and moderate values of mh^2/I_Y. Thus, although no comparison between model and airplane tumbling results is available, it appears that unless an airplane encounters an extrinsic force in flight (similar to that given a model when launched with forced rotation, which is believed to be a rather remote possibility) the center of gravity indicated on the figure as necessary to prevent tumbling may be conservative. Further, references 4 and 5 indicate that the increase in lift due to pitching velocity decreases with either an increase in Reynolds number or Mach number. There is one instance (data unpublished) where a body of near conical shape rotated in a free stream about an axis normal to the axis of symmetry but did not rotate at all when either the Reynolds number or Mach number was increased. In spite of the fact that a cone is not a very efficient lifting device, these results indicate that some scale effect may be expected and that the full-scale airplane may be less prone to tumbling than the model.

Figure 3 presents the results of tumbling investigations for four models whose aspect ratios were 3 or less. For these models, tests were made only from forced rotation, and again the models would not tumble for relatively forward center-of-gravity positions but would tumble for rearward positions.

Comparisons of results in figures 2 and 3 indicates that, for the models of low aspect ratios, further rearward center-of-gravity positions were permissible than for models with large aspect ratio before tumbling tendencies were obtained. These results appear to be consistent with those in reference 2. The reason for the difference due to aspect ratio was not apparent.

Results of tumbling tests of five flat plates are presented in figure 4. These results show separation between conditions of no tumble and those of tumbles similar to those obtained for the models. The center-of-gravity positions for which no tumbles were obtained were farther rearward, however, than were those for the specific models of similar aspect ratios (fig. 2). As previously noted, however, a specific model was said to be capable of tumbling if tumbles occurred for any elevator position which includes elevator set to aid the tumbling rotation. Because the tendency to tumble is greater when the elevators are deflected in the direction of the forced rotation than when the elevators are neutral, and inasmuch as the flat plates had no elevator, the results of tests of the flat plates (with essentially neutral elevator) may therefore be somewhat optimistic with regards to the center-of-gravity position required to prevent tumbling. The differences between the results of tests of flat plates and specific models may also be in part due to the basic physical differences between flat plates and actual airfoil sections. As noted in the appendix, the hysteresis in lift is considered to be the primary motive force in tumbling motions. The results of reference 6 indicate that thin airfoils have less hysteresis in lift than thick airfoil sections. It would appear therefore that flat plates and wings of thin airfoils may generally have less tendency to tumble than wings of thick airfoil sections.

The results obtained with the flat plates indicate that in the region in which tumbling occurred only by forced rotation, quite a number of no-tumbling conditions were also obtained. This is probably due to the fact that the parameters used for the current empirical criterion to obtain separation between tumbling and no-tumbling conditions do not completely dictate this separation and that other factors may have some influence.

Some of the models tested tended to assume motions other than tumbling motion when launched for tumble tests. Such motions as rolling or cart wheeling (rotation about the Z-axis) were experienced. The results of all tumbling tests indicate that the models tend to tumble or rotate about the axis of least moment of inertia and/or aerodynamic damping. If, for example, the moments of inertia about the X and Y body axes were the same, some models may tend to tumble and others to roll, depending on the relative damping. Nonuniform gyrations about all axes may also be possible. No investigations have been made of these specific or different motions. As an example, however, model H, has been observed to roll about the X body axis rather than to tumble. This rolling motion could be stopped by aileron movement against the rolling motion. It is probable that other nonuniform motions which have been observed could be controlled by proper control manipulation inasmuch as the models generally assumed conditions of unstalled flight during the course of the motion. Such nonuniform motions generally occurred when the moment of inertia about the Y-axis was larger than that about the X-axis.

In summary, the separation curves for the specific models (figs. 2 and 3) have been redrawn in figure 5 showing an empirical criterion for the prevention of tumbling. Design of airplanes without horizontal tails in accordance with this criterion should reasonably assure that the airplane will not tumble provided it is within the range of geometric and mass characteristics of the designs presented herein. It appears desirable to make the design fall below the lowest criterion curve (fig. 5); but, should this be impracticable, the design should fall below the separation curve below which tumbles from whip stalls are not likely. Center-of-gravity positions that fall below this line are generally necessary for normal stability.

CONCLUDING REMARKS

The results of tumbling investigations of several models in the Langley 20-foot spinning tunnel have been studied with regard to the design characteristics and loadings that are conducive to tumbling. A preliminary empirical criterion for the prevention of tumbling is presented which indicates center-of-gravity positions and values of other parameters which should prevent tumbling. It appears that further research will be required in order to understand completely the problem of tumbling.

Langley Aeronautical Laboratory
National Advisory Committee for Aeronautics
Langley Air Force Base, Va.

APPENDIX

THEORY OF TUMBLING MOTION

Dupleich has shown in reference 2 that tumbling is caused by a phenomenon associated with a discontinuity in the aerodynamic forces resulting from a rapid change in angle of attack through the stall. Figure 6, taken from reference 6, shows that this phenomenon commonly known as hysteresis can produce large variations in the aerodynamic forces due to rate of change of angle of attack. When the angle of attack is being varied so that a wing is going from an unstalled flow to stalled flow, the flow is altered in such a manner that greater forces result at any given angle of attack than would for a static test at the same angle of attack. Conversely, lesser forces result when a wing is being unstalled.

The mechanics of the tumbling motion may be described by considering the energy produced by the aerodynamic forces. Shown in figure 7 are hypothetical curves of pitching moments against angle of attack which are believed to be reasonable and representative of a flat plate in tumbling equilibrium with the center of gravity at the 50 percent chord. The areas outlined by the moment curves represent the energy resulting from the various moments. The flat plate is used to illustrate the mechanics of tumbling inasmuch as it is bisymmetrical and therefore requires only one-half revolution in pitch to complete a cycle of the pitching moments. There are three separate aerodynamic pitching moments in action during a tumble: the static moment $(M)_\alpha$ which initiates the pitching motion; the moment due to rate of change of angle of attack $(M)_{\dot{\alpha}}$ which supplies the motive energy that causes the pitching motion to accelerate more rapidly; and the moment due to pitch $(M)_q$ which is the damping moment that causes the pitching motion to reach the steady state. At the start of the motion more energy is supplied by $(M)_{\dot{\alpha}}$ than can be absorbed by $(M)_q$, thus

$$\int_0^{\frac{\pi}{2}} \left[(M)_\alpha + (M)_{\dot{\alpha}} + (M)_q\right] d\alpha + \int_{\frac{\pi}{2}}^{\pi} \left[(M)_\alpha + (M)_{\dot{\alpha}} + (M)_q\right] d\alpha > 0 \qquad (1a)$$

This inequality exists until when during the nth cycle of the motion the energy supplied by $(M)_{\dot{\alpha}}$ is exactly equal to the energy absorbed by $(M)_q$ and equilibrium is obtained

$$\int_{n\pi}^{n\pi+\frac{\pi}{2}} \left[(M)_\alpha + (M)_{\dot{\alpha}} + (M)_q\right] d\alpha + \int_{n\pi+\frac{\pi}{2}}^{n\pi+\pi} \left[(M)_\alpha + (M)_{\dot{\alpha}} + (M)_q\right] d\alpha = 0 \qquad (1b)$$

The kinetic energy of the tumbling motion during the nth cycle of the motion or any cycle after equilibrium has been established is equal to the total energy supplied in obtaining equilibrium.

$$\frac{1}{2} I_Y \bar{q}^2 = \int_0^{n\pi} \left[(M)_\alpha + (M)_{\dot{\alpha}} + (M)_q\right] d\alpha \qquad (1c)$$

The energy due to the static moment absorbed by a flat plate or any bisymmetrical section during a cycle will be zero if the path of the center of gravity is along a straight line. Experiment has shown (references 1 and 2) that the deviation of flight path from a straight line is small (flight-path angle is nearly constant) and the flight path therefore may be considered as a straight line. Equations 1 may then be written omitting $(M)_\alpha$. It thus appears that tumbling occurs when the energy supplied by the pitching moment due to rate of change of angle of attack exceeds the energy absorbed due to the damping moment. This condition can exist only if the static moment and the moment of inertia are such as to permit a rate of change of angle of attack that for the given aerodynamic shape will generate sufficient hysteresis in lift. In the case of a wing whose static pitching-moment curve is unsymmetrical more or less hysteresis in lift must be generated to balance the energy resulting from the asymmetry of the static pitching moment.

The flight path of a tumbling wing is determined by the balance of the instantaneous aerodynamic and inertia forces and moments. (See fig. 1.) The equations of motion for the three degrees of freedom are:

$$m \frac{d^2\xi}{dt^2} = W - \left[(D)_\alpha + (D)_{\dot{\alpha}} + (D)_q\right] \sin \gamma + \left[(L)_\alpha + (L)_{\dot{\alpha}} + (L)_q\right] \cos \gamma \qquad (2)$$

$$m \frac{d^2\zeta}{dt^2} = \left[(L)_\alpha + (L)_{\dot{\alpha}} + (L)_q\right] \sin \gamma + \left[(D)_\alpha + (D)_{\dot{\alpha}} + (D)_q\right] \cos \gamma \qquad (3)$$

$$I_Y \frac{d^2\theta}{dt^2} = \left[(M)_\alpha + (M)_{\dot{\alpha}} + (M)_q\right] \qquad (4)$$

Because the variables in equations (2), (3), and (4) are nonlinear and are interdependent, a general solution of the equations is not possible by currently known methods. Because the aerodynamic forces and moment are not constant, the velocity of the center of gravity as well as the rotation about the center of gravity can not be uniform. As previously indicated, however, the resulting flight path will not deviate appreciably from a straight line and therefore $\frac{d\theta}{dt} \approx \frac{d\alpha}{dt}$. In the case of tumbling, this rotation in pitch $\frac{d\alpha}{dt}$ is not small, as in most stability problems, and exceeds all known values for which data have been taken with regard to its effect on lift, drag, and pitching moment. It appears that lift, drag, and pitching-moment data must be obtained throughout the range of values of pitching velocity peculiar to the tumble for any particular airplane in question before a solution to equations (2), (3), and (4) can be obtained. For complete solution of the tumble problem more knowledge will be required about the mechanics of, and the parameters which control, hysteresis and damping at values of pitching velocity peculiar to the tumble.

REFERENCES

1. Stone, Ralph W., Jr., and Bryant, Robert L.: Summary of Results of Tumbling Investigations Made in the Langley 20-Foot Free-Spinning Tunnel on 14 Dynamic Models. NACA RM L8J28, 1948.

2. Dupleich, Paul: Rotation in Free Fall of Rectangular Wings of Elongated Shape. NACA TM 1201, 1949.

3. Zimmerman, C. H.: Preliminary Tests in the N.A.C.A. Free-Spinning Wind Tunnel. NACA Rep. 557, 1936.

4. Harper, Paul W., and Flanigan, Roy E.: The Effect of Rate of Change of Angle of Attack on the Maximum Lift of a Small Model. NACA TN 2061, 1950.

5. Spreiter, John R., Galster, George M., and Blair, William K.: Effect of Mach and Reynolds Numbers on Maximum Lift Coefficient Obtainable in Gradual and Abrupt Stalls of a Pursuit Airplane Equipped with a Low-Drag Wing. NACA MR A5G06, Bur. Aero., 1945.

6. Farren, W. S.: The Reaction on a Wing Whose Angle of Incidence Is Changing Rapidly. Wind Tunnel Experiments with a Short Period Recording Balance. R. & M. No. 1648, British A.R.C., 1935.

TABLE I.- DIMENSIONAL CHARACTERISTICS OF MODELS TESTED

[Model values are presented in terms of full-scale values]

Model	Scale	Span (ft)	Area (ft²)	Aspect ratio	Taper ratio	Sweep 1/4 c (deg)	M.A.C. (in.)	L.E. M.A.C. aft L.E. root (in.)
A	1/16	23.30	427.00	1.27	-----	0.0	238.00	10.02
B	1/20	60.00	490.00	7.36	0.248	21.9 back	109.80	69.70
C	1/57.33	172.00	4020.00	7.36	0.248	21.9 back	315.00	200.00
D	1/17.8	54.00	356.00	8.20	0.376	15.0 fwd	85.82	-29.10 (fwd)
E	1/17.55	38.67	496.00	3.01	0.600	35.0 back	157.00	83.56
F	1/20	51.67	362.00	7.37	0.249	22.0 back	94.50	60.10
[1]G	1/20	44.58	517.40	3.84	1.000	30.0 back	140.00	77.20
H	1/20	29.42	375.00	2.31	0.000	37.6 back	203.90	101.90
[1]I	1/30	30.00	673.20	1.34	1.000	45.0 back	272.00	88.80
J	1/16	39.00	293.31	5.19	0.253	24.9 back	102.30	49.30
K	1/30	134.00	1800.00	10.00	0.167	11.2 back	190.80	82.80
L	1/60	290.00	7920.00	10.60	0.200	0.6 fwd	375.60	20.88
M	1/20	26.83	200.00	3.60	0.455	38.1 back	93.68	62.48
[2]N	1/20	50.00	250.00	10.00	1.000	0.0	60.00	0.00
[2]O	1/20	45.00	225.00	9.00	1.000	0.0	60.00	0.00
[2]P	1/20	40.00	200.00	8.00	1.000	0.0	60.00	0.00
[2]Q	1/20	35.00	175.00	7.00	1.000	0.0	60.00	0.00
[2]R	1/20	40.00	266.70	6.00	1.000	0.0	80.00	0.00

NACA

[1]Research models.

[2]Flat plates.

Others - models of specific airplanes.

TABLE II.- MASS, PITCHING-MOMENT CHARACTERISTICS, AND TUMBLE RESULTS OF MODELS TESTED

[Model values are presented in terms of full-scale values]

Model	Typical C_M against C_L curves	Loading: Weight (lb)	Loading: μ_b Sea level	Loading: μ_b Altitude (ft)	Loading: I_Y (slug-feet²)	Center-of-gravity location (percent $\bar{c}$)	$\frac{mb^2}{I_Y}$	Tumble result (a)
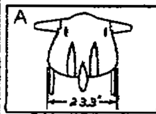	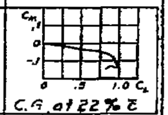	16,858	22.05	15,000 35.08	19,367	26.3	0.76	+
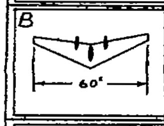	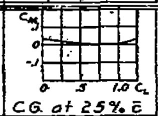	6,526	2.91	15,000 4.62	2,274	29.0	.33	○
		6,694	2.98	4.73	2,679	24.0	.44	□
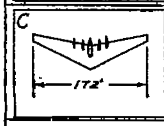	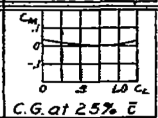	155,000	2.93	20,000 5.50	433,500	27.5	.38	○
		155,000	2.93	5.50	433,500	20.0	.69	+
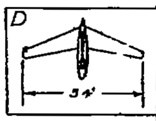	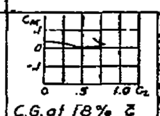	3,846	2.61	15,000 4.13	4,369	18.0	.12	□
		3,507	2.38	3.79	4,275	16.0	.15	□
		3,846	2.61	4.13	4,864	13.0	.17	+
		3,846	2.61	4.13	3,844	23.0	.12	□
		7,886	5.35	8.51	4,738	18.0	.27	□
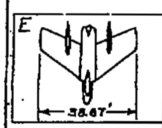	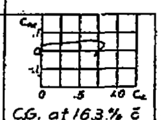	14,517	9.89	15,000 15.72	22,943	16.7	.38	+
		14,484	9.87	15.68	23,810	24.0	.21	+
		14,484	9.86	15.68	25,412	22.6	.22	+
		14,616	9.95	15.82	29,935	32.6	.08	□
		14,549	9.91	15.75	29,762	37.6	.04	□
		13,955	9.49	15.09	18,991	38.7	.05	□
		14,857	10.11	16.07	24,387	21.6	.26	+
		14,872	10.11	16.07	17,663	30.6	.16	□
		14,872	10.11	16.07	35,954	30.6	.08	□
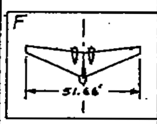	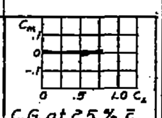	4,766	3.36	20,000 6.24	1,920	21.2	.40	□
		4,766	3.33	6.24	2,159	19.2	.41	□
		4,673	3.25	6.12	2,051	17.3	.47	+
		3,691	2.58	4.85	2,251	20.0	.29	□
		3,691	2.58	4.85	2,133	16.2	.38	□
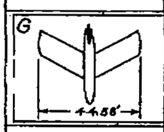	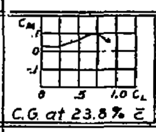	7,832	4.43	20,000 8.32	3,432	30.7	.36	□
		7,832	4.43	8.32	4,884	17.1	.73	+
		7,832	4.43	8.32	7,706	7.9	.76	+
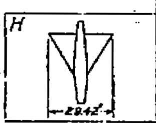	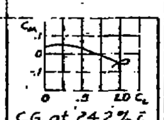	11,648	13.80	15,000 22.00	27,619	24.0	.26	+
		12,153	14.50	22.84	28,500	30.0	.15	□
		12,153	14.50	22.84	26,800	35.0	.09	□
		16,082	19.20	30.40	65,000	24.0	.15	□
		17,302	20.60	32.70	61,000	29.9	.07	□
		12,130	14.50	22.80	25,900	41.6	.03	□

(a) Key
○ Tumble from a whip stall.
□ Tumble when given forced rotation.
\+ No tumble.

NACA

[redacted]

TABLE II.- MASS, PITCHING-MOMENT CHARACTERISTICS, AND TUMBLE RESULTS OF MODELS TESTED - Continued

Model	Typical C_M against C_L curves	Loading: Weight (lb)	Loading: μ_b Sea Level	Loading: μ_b Altitude (ft)	Loading: I_Y (slug-feet^2)	Center-of-gravity location (percent $\bar{c}$)	$\frac{mk^2}{I_Y}$	Tumble result (a)
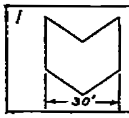	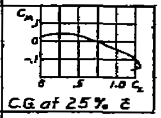	10,453	6.75	15,000 10.70	10,816	35.4	0.33	+
		10,453	6.75	10.70	10,852	38.3	.21	□
		10,453	6.75	10.70	11,382	42.3	.09	□
		15,811	10.00	16.10	10,757	35.7	.48	+
		15,811	10.00	16.10	11,022	39.2	.27	+
		15,811	10.00	16.10	10,757	35.4	.50	+
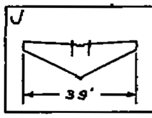	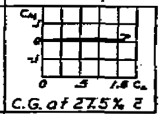	4,642	5.31	15,000 8.42	1,030	25.1	.63	□
		9,000	10.26	16.36	1,520	26.8	.73	□
		13,291	15.15	24.14	1,925	26.8	.85	□
		4,642	5.31	8.42	1,030	38.3	.14	O
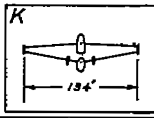	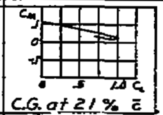	60,600	3.28	------	232,708	21.0	.17	□
		60,600	3.28	------	232,708	24.0	.14	□
		60,600	3.28	------	232,708	25.0	.13	O
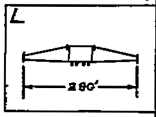	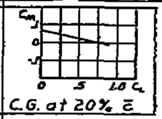	317,000	1.80	20,000 3.39	10,018,370	26.0	.05	□
		317,000	1.80	3.39	10,018,370	27.5	.05	□
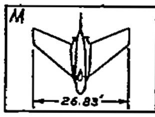	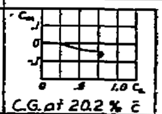	6,815	10.44	15,000 16.60	2,749	19.9	.43	□
		6,815	10.44	16.60	2,880	25.6	.27	□
		5,820	8.93	14.20	2,640	15.9	.49	+
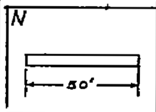	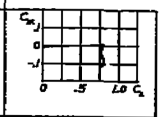	3,038	3.18	10,000 4.31	127	31.4	.69	+
		3,038	3.18	4.31	94	35.8	.53	□
		3,038	3.18	4.31	74	39.4	.39	O
		5,363	5.58	7.56	77	33.6	1.44	+
		5,363	5.58	7.56	69	37.3	.96	□
		5,363	5.58	7.56	64	41.0	.53	O
		5,363	5.58	7.56	663	30.1	.25	+
		5,266	5.48	7.43	545	40.0	.08	□
		5,363	5.58	7.56	503	41.5	.06	O
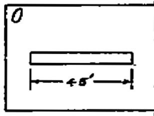	Similar to model N	1,775	2.28	10,000 3.09	84	32.0	.53	+
		1,775	2.28	3.09	68	37.0	.34	□
		1,775	2.28	3.09	62	40.0	.24	O
		2,610	3.36	4.55	63	30.0	1.28	+
		2,790	3.59	4.86	72	34.0	.74	□
		2,790	3.59	4.86	64	38.0	.53	O
		3,584	4.61	6.24	54	33.0	1.52	+
		3,584	4.61	6.24	48	36.0	1.04	□
		3,584	4.61	6.24	45	40.0	.72	O
		5,675	7.31	9.90	682	27.0	.36	□
		5,675	7.31	9.90	628	30.0	.30	□
		5,675	7.31	9.90	460	44.0	.04	O

(a) Key
O Tumble from a whip stall.
□ Tumble when given forced rotation.
+ No tumble.

NACA

TABLE II.- MASS, PITCHING-MOMENT CHARACTERISTICS, AND TUMBLE RESULTS OF MODELS TESTED - Concluded

Model	Typical C_M against C_L curves	Loading: Weight (lb)	Loading: μ_b Sea Level	Loading: μ_b Altitude (ft) 10,000	Loading: I_Y (slug-feet^2)	Center-of-gravity location (percent $\bar{c}$)	$\frac{mk^2}{I_Y}$	Tumble result (a)
		1,370	2.24	2.99	48	32.0	0.67	+
		1,370	2.24	2.99	43	35.0	.52	□
		1,370	2.24	2.99	39	38.0	.40	○
P 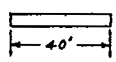	Similar to model N	2,324	3.78	5.12	46	32.0	1.23	+
		2,324	3.78	5.12	40	36.0	.88	□
		2,324	3.78	5.12	37	39.0	.55	○
		3,246	5.33	7.21	42	36.0	1.12	+
		3,246	5.33	7.21	39	40.0	.63	○
		5,064	8.25	11.17	523	28.0	.37	+
		5,064	8.25	11.17	436	30.0	.35	□
		5,064	8.25	11.17	400	40.0	.10	□
		5,064	8.25	11.17	412	44.0	.05	○
		1,240	2.64	3.58	40	35.0	.50	+
		1,240	2.64	3.58	36	38.0	.34	□
		1,240	2.64	3.58	34	40.0	.26	○
		2,038	4.36	5.85	37	37.0	.72	+
Q 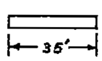	Similar to model N	2,038	4.36	5.85	34	40.0	.47	□
		2,038	4.36	5.85	31	44.0	.22	○
		2,805	5.97	8.08	41	33.0	1.57	+
		2,805	5.97	8.08	38	37.0	1.03	□
		2,805	5.97	8.08	34	40.0	.65	○
		4,428	9.47	12.82	462	28.0	.36	+
		4,428	9.47	12.82	435	30.0	.31	□
		4,428	9.47	12.82	361	40.0	.11	□
		4,428	9.47	12.82	339	44.0	.03	○
		1,580	1.94	2.62	114	34.0	.45	+
		1,580	1.94	2.62	105	37.0	.37	□
		1,580	1.94	2.62	99	38.0	.29	○
R 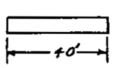	Similar to model N	2,506	3.08	4.17	102	36.0	.64	□
		2,506	3.08	4.17	95	39.0	.46	○
		3,428	4.20	5.66	105	36.0	.95	+
		3,428	4.20	5.66	136	38.0	.50	□
		3,428	4.20	5.66	92	41.0	.45	○
		5,272	6.46	8.76	1083	26.0	.39	□
		5,272	6.46	8.76	823	36.0	.16	□
		5,272	6.46	8.76	800	38.0	.13	○

(a) Key
○ Tumble from a whip stall.
□ Tumble when given forced rotation.
\+ No tumble.

NACA

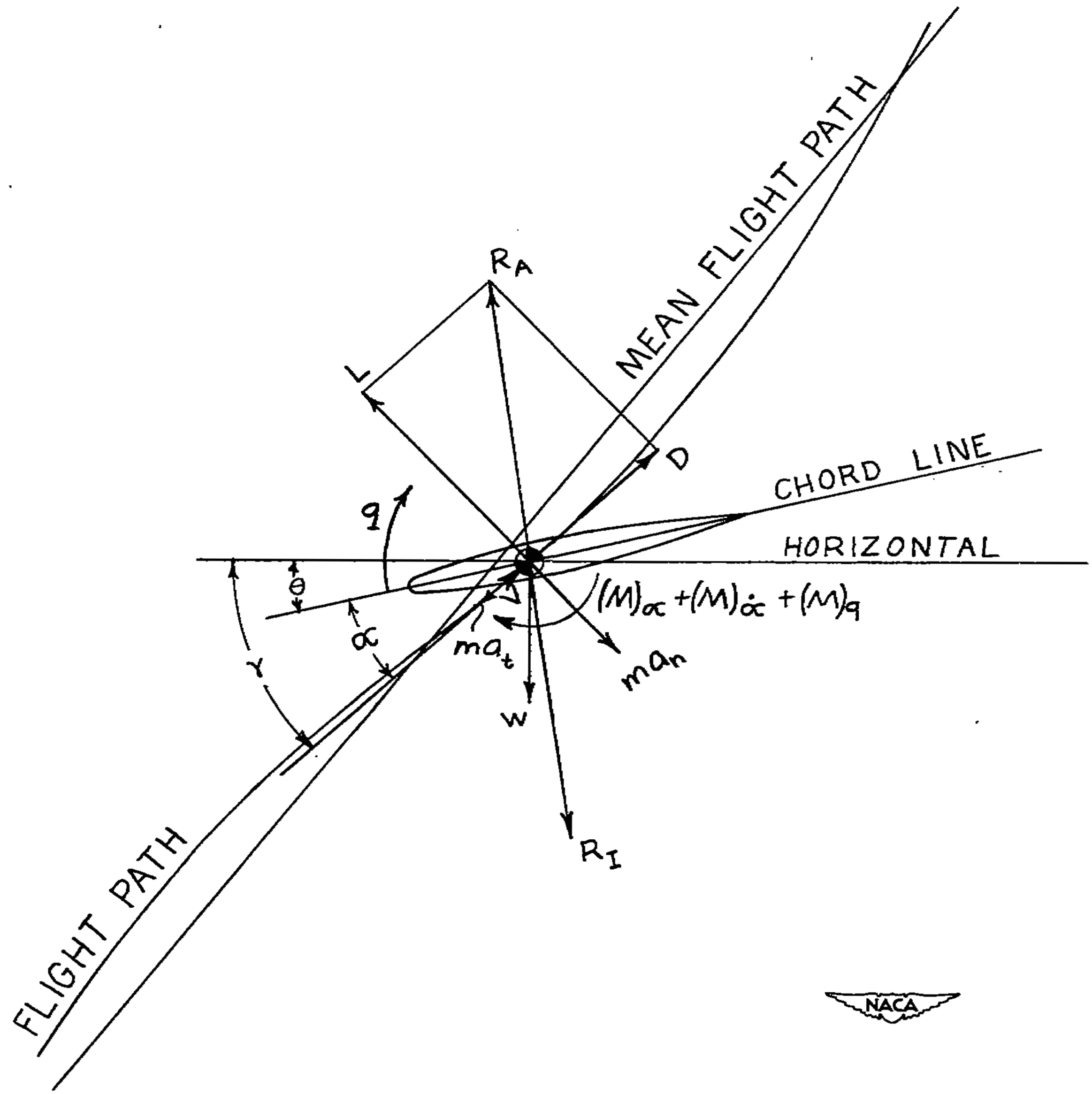

Figure 1.- Angular and vectorial relationships for a tumbling wing.

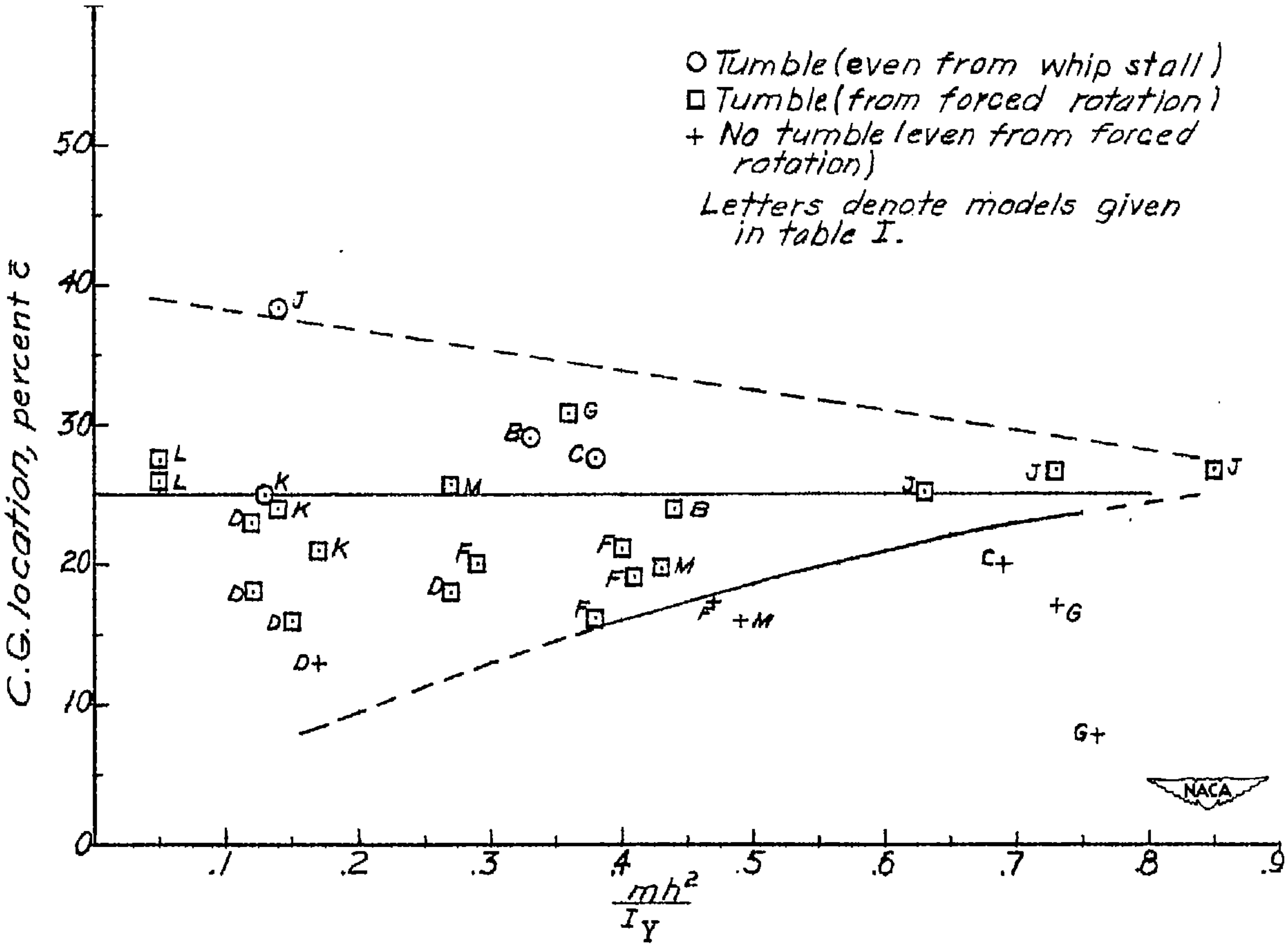

Figure 2.- Tumbling tendencies of airplane models having no horizontal tail and whose aspect ratios are between 3 and 11.

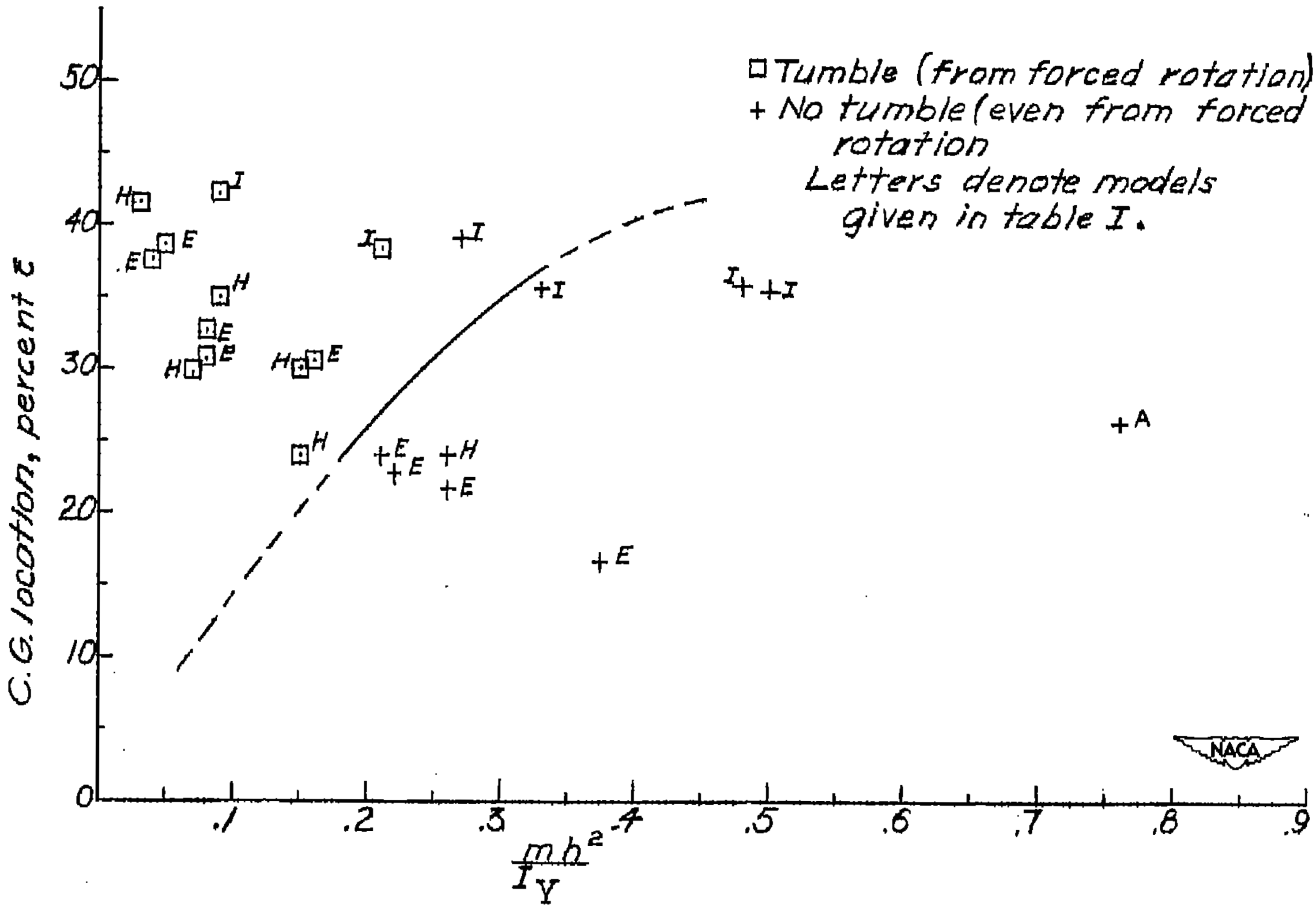

Figure 3.- Tumbling tendencies of airplane models having no horizontal tail and whose aspect ratios are between 1 and 3.

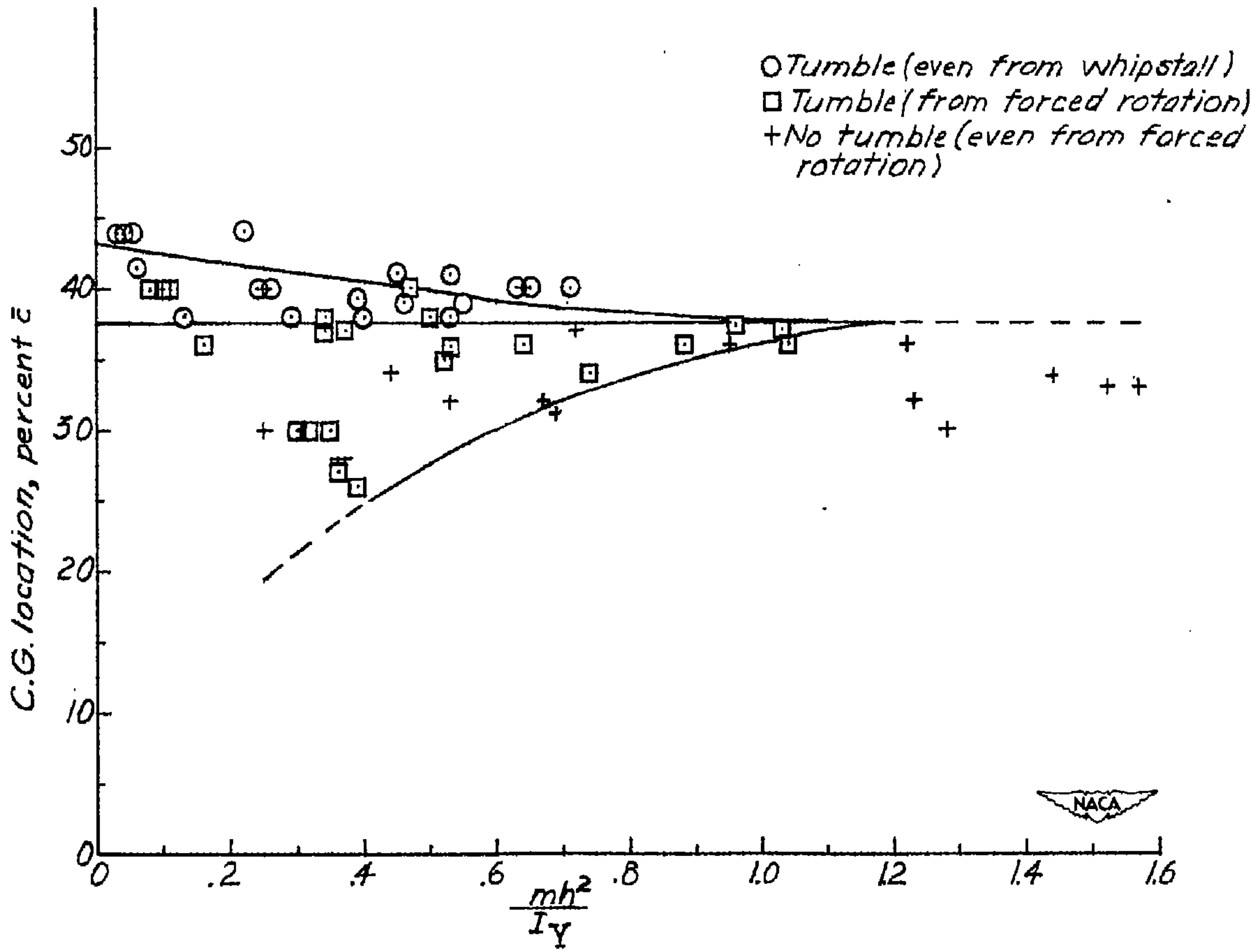

Figure 4.- Tumbling tendencies of flat plates whose aspect ratios are between 6 and 10.

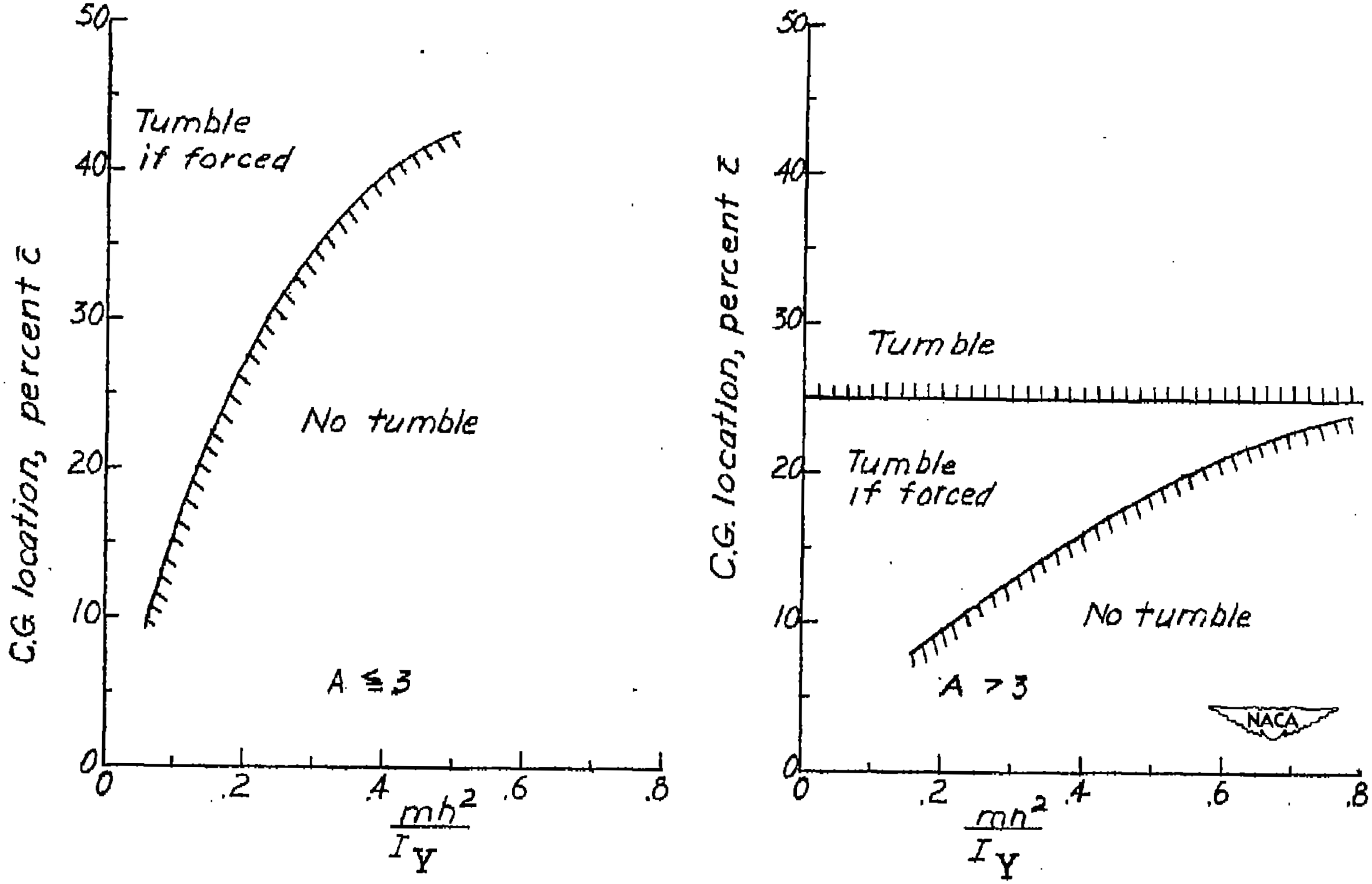

Figure 5.- Preliminary design requirements for the prevention of tumbling of airplanes having no horizontal tail.

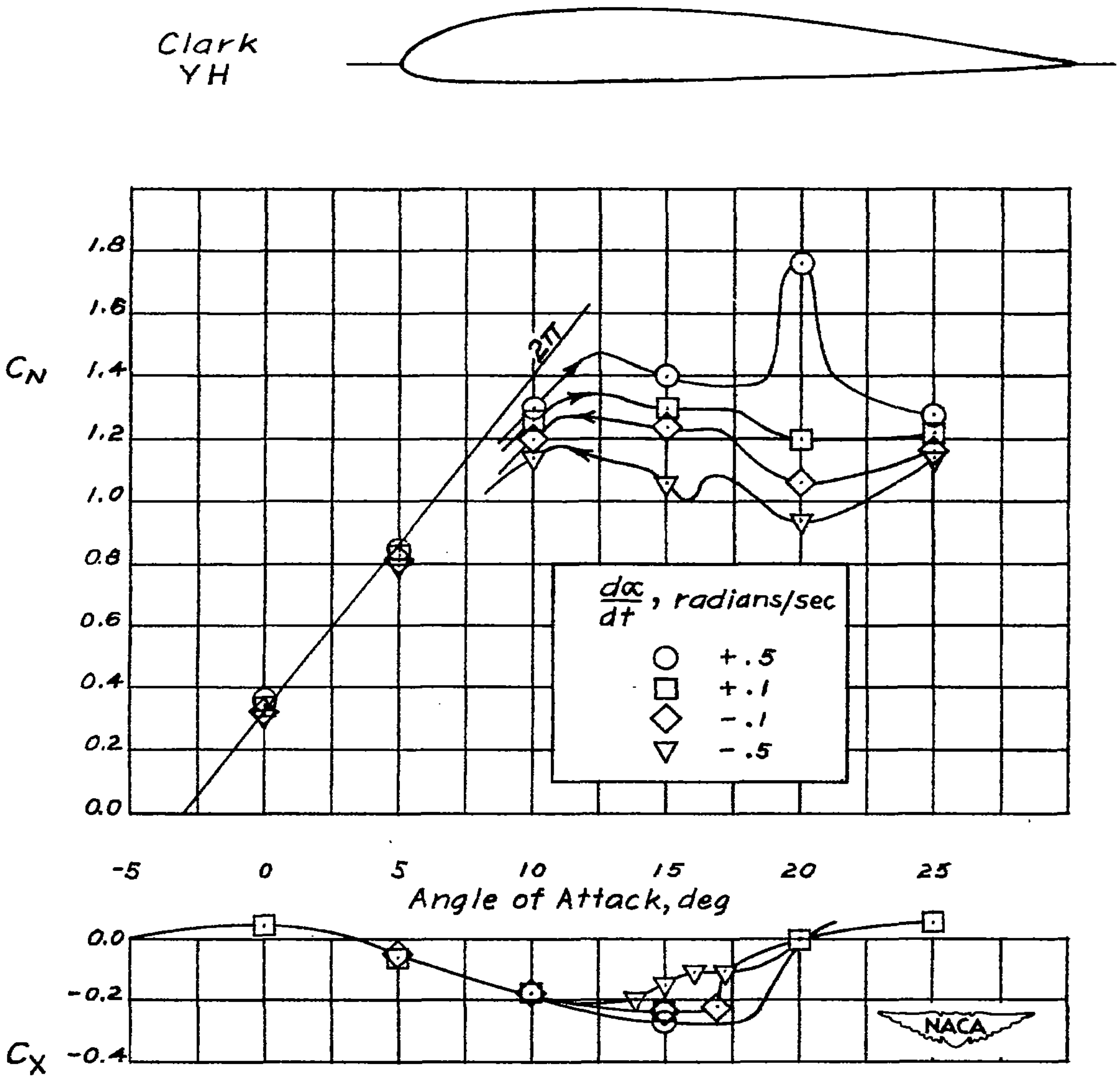

Figure 6.- Normal- and longitudinal-force coefficients of a Clark YH wing whose angle of attack is being varied rapidly at an airspeed of 37.5 feet per second.

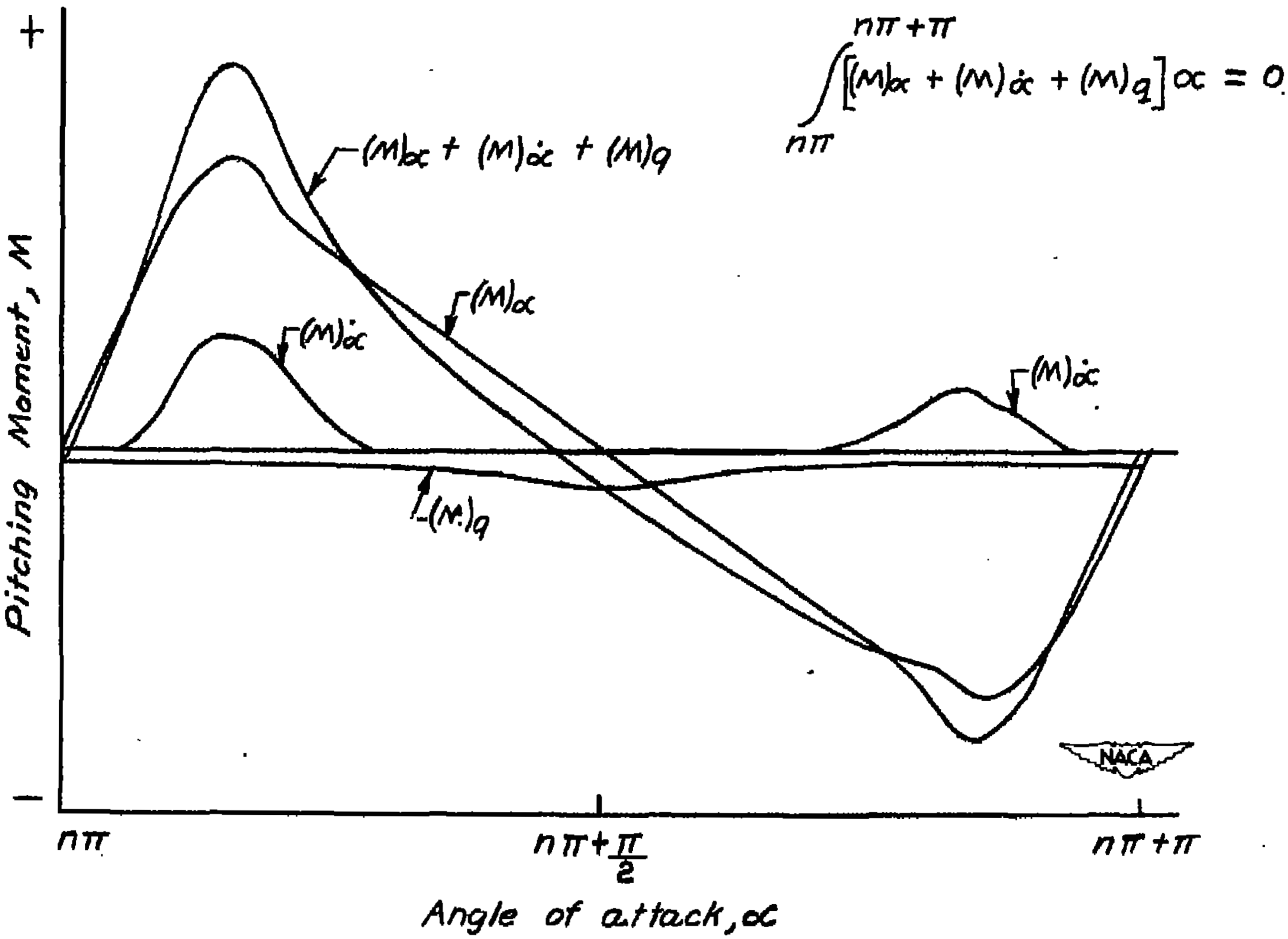

Figure 7.- Hypothetical curves of pitching-moment distribution for a flat plate in tumbling equilibrium with the center of gravity at the centroid. The areas above and below the zero moment represent the energy gained and lost, respectively, during a half-revolution.